11th World Congress on Computational Mechanics (WCCM XI)
5th European Conference on Computational Mechanics (ECCM V)
6th European Conference on Computational Fluid Dynamics (ECFD VI)
E. Oñate, J. Oliver and A. Huerta (Eds)

NUMERICAL PREDICTIONS OF VISCOELASTIC FLOWS WITH AN ALGEBRAIC EXTRA-STRESS MODEL

DAIANE I. DOLCI*, GILCILENE S. PAULO* AND GILMAR MOMPEAN†

* Faculdade de Ciências e Tecnologia (FCT)
UNESP - Univ Estadual Paulista
Campus de Presidente Prudente, Rua Roberto Simonsen 305, 19060-900 Presidente Prudente/SP, Brazil
e-mail: daia.dolci@gmail.com, gilcilene@fct.unesp.br, web page: http://www.fct.unesp.br/

† Université des Sciences et Technologies de Lille
PolytechLille, Laboratoire de Mécanique de Lille, URM-CNRS 8107
Cité Scientifique, 59655 Villeneuve dAscq Cedex, France
e-mail: gilmar.mompean@polytech-lille.fr - Web page: www.lml.univ-lille1.fr

Key words: Viscoelastic Flows, Algebraic and Differential PTT Model, CPU Time, Planar Contraction

Abstract. Numerical simulation of viscoelastic flows using Phan-Thien-Tanner (PTT) [1] differential constitutive equation, and an algebraic extra-stress model (AESM) proposed by G. Mompean [2] are presented in this work. In order to evaluate the perform of the AESM and show that it can cope with complex flows, two problems are studied: fully-developed channel flow and the flow through a 4:1 planar contraction at low Reynolds number. The governing equations are solved using a Marker-and-Cell type method on a staggered grid [3]. The momentum equation is integrated by the implicit scheme while the algebraic PTT equation is solved explicitly by a forward Euler method. The accuracy of the numerical method is verified by comparing numerical results of fully-developed channel flow with the corresponding analytic solutions. The planar contraction problem is employed to assess whether the algebraic model is able to predict the viscoelastic flow displaying the same behavior of the differential PTT model. Moreover, to show the advantages of the algebraic extra-stress model (AESM) over the differential PTT model, a study of the computational effort has been carried out.

1 INTRODUCTION

The development of the numerical techniques to solve Navier-Stokes equations coupled with constitute equations for modeling viscoelastic flows has been an area of great interest for many researchers. Although the computers have been improved on their capabilities of

processing and storing, the researchers are still having to deal with computational effort when considering numerical simulation of complex flows, as for example viscoelastic fluids. The algebraic extra-stress model (AESM) proposed by Mompean and collaborators in [4] to model viscoelastic flows has better perform in terms of computational effort, saving cpu time to obtain numerical solutions, when compared with the classical differential constitutive equations.

First, the AESM model was developed to approximate the Oldroyd-B differential model [4], and numerical results demonstrating its abilities can be found in [4] and [2]. In the paper [2], Mompean extended the AESM model to approximate PTT differential model [1]. However, numerical results comparing the prediction of this kind of approach with the classical differential model were not presented. Therefore, the present work deal with numerical studies of the PTT using the algebraic extra-stress approach, including the validation and the convergence of the numerical methodology. The advantages of the algebraic model over the differential model in terms of computational effort and numerical predictions of viscoelastic flows with PTT algebraic model are also presented.

This work is organized as follow: section 2 describes the governing equations and summaries the strategy for getting the AESM model, in section 3 a brief description of the numerical methodology is presented and finally section 4 is dedicated to numerical simulations of two problems, fully-developed channel flow and the flow through a 4:1 planar contraction at low Reynolds number.

2 GOVERNING EQUATIONS AND AN ALGEBRAIC EXTRA-STRESS MODEL

The governing equations for modeling isothermal incompressible viscoelastic flows are the incompressibility condition and the equation of motion expressed in dimensionless form by Eqs.(1) and (2), respectively.

$$\nabla \cdot \mathbf{u} = 0 \ , \tag{1}$$

$$\frac{\partial \mathbf{u}}{\partial t} + \nabla \cdot (\mathbf{uu}) = -\nabla p + \frac{\beta}{Re}\nabla^2 \mathbf{u} + \nabla \cdot \mathbf{T} \ , \tag{2}$$

where t is the time, $\mathbf{u}$ is the velocity vector, p is the pressure, $\mathbf{T}$ is the non-Newtonian extra-stress tensor. The non-dimensional Reynolds number, $Re = \dfrac{\rho U L}{\eta_0}$, is defined considering the constants L, U and ρ which denote typical scalings for length, velocity and density, respectively. The amount of Newtonian solvent is controlled by the dimensionless coefficient $\beta = \dfrac{\eta_S}{\eta_0}$, where $\eta_0 = \eta_S + \eta_P$ represents the total viscosity at zero shear while η_S and η_P represent the Newtonian and polymeric viscosities.

To represent viscoelastic phenomena there are several constitutive equations (see, for instance, [5, 6]). In this work, the differential Phan-Thien-Tanner (PTT) model, given by Eq. (3), is also considered to explore numerically the algebraic extra-stress model (AESM) proposed by Mompean [2].

The differential PTT constitute equation is given by

$$f(I_{\mathbf{T}})\mathbf{T} + Wi\,\overset{\triangledown}{\mathbf{T}} = 2\frac{(1-\beta)}{Re}\mathbf{S}\,, \tag{3}$$

where $I_{\mathbf{T}} = \{\mathbf{T}\}$ is the trace of $\mathbf{T}$, $\mathbf{S} = 1/2\left[\nabla\mathbf{u} + \nabla\mathbf{u}^{\top}\right]$ is the deformation tensor, the function $f = f(I_{\mathbf{T}}) = 1 + \varepsilon\dfrac{Re\;Wi}{(1-\beta)}I_{\mathbf{T}}$ is used in the linear form, ε is a constant parameter of the PTT model. Wi is the Weissenberg number difined as $Wi = \lambda U/L$, where λ is the relaxation time. The symbol $\overset{\triangledown}{(\cdot)}$ represents the upper convected frame-invariant derivative,

$$\overset{\triangledown}{\mathbf{T}} = \frac{D\mathbf{T}}{Dt} - \nabla\mathbf{u}\cdot\mathbf{T} - \mathbf{T}\cdot\nabla\mathbf{u}^{\top}\,.$$

D/Dt represents the material derivative and $(\cdot)^{\top}$ the transpose matrix, pointing out that the element, $(\nabla\mathbf{u})_{ij}$, of the velocity gradient matrix is considered $(\nabla\mathbf{u})_{ij} = \partial u_i/\partial x_j$.

Below is presented a summary of the process to derive the AESM model according to [2] and [4] for two-dimensional flows.

Defining the rotation tensor as $\mathbf{W} = 1/2\left(\nabla\mathbf{u} - \nabla\mathbf{u}^{\top}\right)$, the Eq. (3) can be written as,

$$\frac{D\mathbf{T}}{Dt} = -\frac{f}{Wi}\mathbf{T} + \frac{2(1-\beta)}{Re\;Wi}\mathbf{S} + (\mathbf{ST} + \mathbf{TS}) - (\mathbf{TW} - \mathbf{WT})\,. \tag{4}$$

Using the deviatoric tensor:

$$\mathbf{\Gamma} = \mathbf{T} - \frac{I_{\mathbf{T}}}{3}\mathbf{I}\,, \tag{5}$$

where $\mathbf{I}$ is the identity tensor, equation (4) can be expressed in terms of the tensor $\mathbf{\Gamma}$ as

$$\frac{D\mathbf{\Gamma}}{Dt} = -\frac{f}{Wi}\mathbf{\Gamma} + (\mathbf{S\Gamma} + \mathbf{\Gamma S} - \frac{2}{3}\{\mathbf{\Gamma S}\}\mathbf{I}) - (\mathbf{\Gamma W} - \mathbf{W\Gamma}) + 2\left(\frac{(1-\beta)}{Re\;Wi} + \frac{I_{\mathbf{T}}}{3}\right)\mathbf{S}\,. \tag{6}$$

Note that the Eq. (6) depends on the trace of $\mathbf{T}$ and an evolution equation for solving $I_{\mathbf{T}}$ is obtained straightaway from Eq. (4),

$$\frac{DI_{\mathbf{T}}}{Dt} = -\frac{f}{Wi}I_{\mathbf{T}} + 2\{\mathbf{\Gamma S}\}\;. \tag{7}$$

Therefore, to solve the differential equation (3) is equivalent to solve the equations (6) and (7).

In order, to obtain the extra-stress algebraic model, two hypotheses of slow variation of the deviatoric tensor were studied by Mompean and co-workers in [4]. One of them guarantee a consistent approximation for two-dimensional viscoelastic flows which provides the following explicit algebraic equation,

$$\mathbf{\Gamma} = \frac{\{\mathbf{\Gamma S}\}}{\{\mathbf{S}^2\}}\mathbf{S} - \frac{1}{2}\frac{I_{\mathbf{T}}}{\{\mathbf{S}^2\}}\left[(\mathbf{SW} - \mathbf{WS}) - 2\left(\mathbf{S}^2 - \frac{1}{3}\{\mathbf{S}^2\}\mathbf{I}\right)\right], \tag{8}$$

where

$$\{\mathbf{\Gamma S}\} = \sqrt{\left(\frac{(1-\beta)}{Re\ Wi} + \frac{I_{\mathbf{T}}}{2}\right) I_{\mathbf{T}}\{\mathbf{S}^2\} + \frac{1}{2}{I_{\mathbf{T}}}^2\{\mathbf{W}^2\}}\ . \tag{9}$$

Therefore, instead of solving three differential equations for the components of the non-Newtonian extra-stress tensor from Eq. (3), with the algebraic transformation only one differential equation must be solved, $I_{\mathbf{T}}$ from Eq. (7). To update the components of the non-Newtonian extra-stress tensor $\mathbf{T}$, the functions $\{\mathbf{\Gamma S}\}$ and $\mathbf{\Gamma}$ given respectively by Eqs. (9) and (8) are calculated algebraically. This procedure allows to obtain each component of $\mathbf{T}$ from Eq. (5).

3 A BRIEF DESCRIPTION OF THE NUMERICAL METHODOLOGY

The numerical methodology is based on GENSMAC (GENeralized Simplified Marker-And-Cell) [3] methodology extending its numerical applicabilities for viscoelastic flows (see for instance, [7, 8, 9]). Equations (1), (2) and (7) are discretized on a uniform 2D Cartesian $\delta x \times \delta y$ staggered grid using the finite difference method. To calculate the numerical solution at the time $t_{n+1} = t_n + \delta t$, the temporal integration of the momentum equation is done by implicit method, apart from the advectives terms and the non-Newtonian extra-stress tensor which are taken at the time t_n and the evolution equation for $I_{\mathbf{T}}$ is solved by forward Euler method. The spacial approximation is basically second order, a convergent and universally bounded interpolation scheme for the treatment of advection (CUBISTA) is employed [10] and the spacial derivatives are approximated by central difference schemes.

As initial condition for the variables, their spacial distribution at time t_0 are $\mathbf{u} = \mathbf{0}$ and $I_{\mathbf{T}}$=1.0e-12. Note that, it is not possible to start with $I_{\mathbf{T}} = 0$ because Eq. (7), which depends on the Eq. (9), leads to a null solution. On the rigid boundaries is imposed the no-slip condition, $\mathbf{u} = \mathbf{0}$ and hence, the calculation of the $I_{\mathbf{T}}$ on these boundaries takes it into account. On the exit boundaries, the homogeneous Neumann condition, $\dfrac{\partial \mathbf{u}}{\partial n} = \mathbf{0}$ and $\dfrac{\partial I_{\mathbf{T}}}{\partial n} = 0$, where n is the unit normal vector to the boundary considered. The inlet conditions will be treated in the next sections.

4 NUMERICAL PREDICTIONS AT LOW REYNOLDS NUMBERS

In this section, numerical results of two problems will be discuss: fully-developed channel flow and the flow through a 4:1 planar contraction. The accuracy of the numerical method presented in the previous section is verified by comparing numerical results of fully-developed channel flow with the corresponding analytic solutions. A mesh refinement will be presented for studying the convergence, the spacial order of the methodology and the advantages of the algebraic extra-stress model (AESM) over the differential PTT model. The 4:1 planar contraction problem will be employed to assess the capability of

the algebraic model to predict numerically the viscoelastic flows, comparing it with the numerical predictions obtained by differential PTT model.

4.1 Fully-developed channel flow

Consider the confined flows between horizontal parallel plates under the initial and boundary conditions above-mentioned until they reach the stead state. On the inlet, the analytic solutions for fully-developed channel flow of the PTT fluid with a Newtonian solvent derived by Cruz and Pinho in [11] was imposed. The following data were employed: the inlet $L = 1$m, channel length $10L$, Re=1.0e-2, $Wi = 0.2$, $\beta = 0.6$, $\varepsilon = 0.5$. To analyse the convergence of the methodology on this problem we computed the numerical solution on four meshes: M1: 10×100 cells ($\delta x = \delta y = 0.1$), M2: 20×200 cells ($\delta x = \delta y = 0.05$), M3: 40×400 cells ($\delta x = \delta y = 0.025$), M4: 60×600 cells ($\delta x = \delta y = 1/60$).

The numerical solution was kept in a cross section at the middle of the channel ($x = 5L$) when the steady state was reached. The comparisons of the numerical and analytic solutions are displayed in the Figs. 1(a)-1(c) which describe the profiles of the components of the extra-stress tensor, T^{xy} and T^{xx}, and the component u of the streamwise velocity.

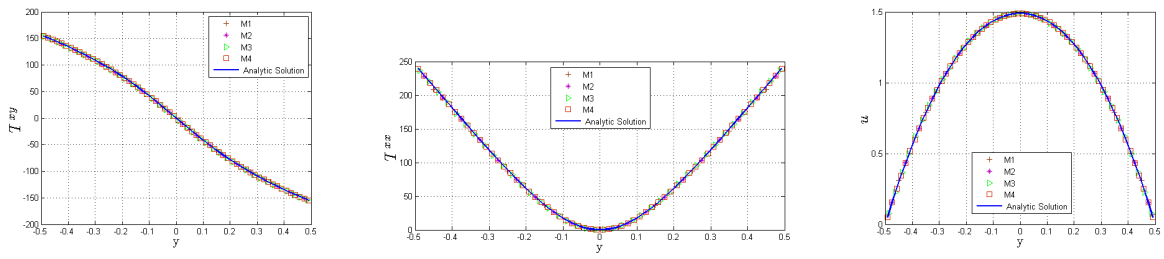

(a) $T^{xy}(y)$ (b) $T^{xx}(y)$ (c) $u(y)$

Figure 1: Symbols represent numerical solutions and continue lines represent analytic solutions of the components T^{xy} (a), T^{xx} (b) and velocity u (c) at the cross section $x = 5L$.

The convergence of the numerical methodology was analysed by calculating the relative error of the numerical solution considering the analytic solution as reference solution. The relative error was calculated from L_1 norm,

$$Error(\text{NumSol}) = \sum_{j=1}^{L/\delta y} |\text{AnalySol} - \text{NumSol}| \Big/ \sum_{j=1}^{L/\delta y} |\text{AnalySol}|.$$

and the results can be seen in Table 1. From Table 1, it can be seen that the spatial order of the numerical methodology is approximately 2.

4.1.1 Computational effort

Herein, it is shown the advantages of the algebraic PTT model over the differential model. In order to probe that, it was carried out several simulations and mesh refinements

Table 1: Relative errors calculated at the middle of the channel for each mesh employed.

Error(T^{xy})	M1	M2	M3	M4
Algebraic	8.091567e-3	2.098316e-3	5.315781e-4	2.370212e-4
Differential	8.093974e-3	2.097720e-3	5.311771e-4	2.370205e-4
Error(T^{xx})				
Algebraic	1.758150e-2	4.516545e-3	1.139792e-3	5.078188e-4
Differential	1.758150e-2	4.516409e-3	1.139735e-3	5.067681e-4
Error(u)				
Algebraic	6.027530e-3	1.597944e-3	4.078612e-4	1.822645e-4
Differential	6.027530e-3	1.597939e-3	4.078589e-4	1.822788e-4

for each one were considered to study the perform in terms of the processing time, for both algebraic and differential PTT models.

Three simulations, S1, S2 and S3, were chosen and one more mesh (M5: 80×800 cells ($\delta x = \delta y = 0.0125$)) among those used in the previous section was considered. In every simulation the Reynolds number is Re= 1.0e-2. The parameters of the numerical simulations were: $Wi = 0.2$, $\varepsilon = 0.5$ and $\beta = 0.7$ for S1; $Wi = 0.4$, $\varepsilon = 0.5$ and $\beta = 0.6$ for S2 and $Wi = 0.2$, $\varepsilon = 0.4$ and $\beta = 0.6$ for S3.

The processing times for each numerical simulation on every mesh are exhibited in Table 2 and reveal that the algebraic model is faster than differential model when refined meshes are used. For the coarse meshes considered (M1, M2 and M3), the cpu time of the algebraic model is closed to the cpu time of the differential model. The PTT-AESM was able to predict the flow using a very fine mesh (M5), and the differential model did not converge for this case.

4.2 4:1 Planar contraction

The comparisons between numerical results from the PTT differential and the PTT algebraic models for the flows throughout a 4:1 planar contraction is presented in this section. For this geometry, the following parameters were considered: smaller channel width $L = 0.5$m, inlet height: $4L = 2.0$m, the distance from inlet to outlet: 6.0m, such as, the entry length is 3.0m and the outlet length is 3.0m. A creeping flow was assumed with a low Reynolds number Re=1.0e-2.

Figure 2 compares the contours of the difference $T^{xx} - T^{yy}$ and of the component T^{xy} between differential and algebraic models. For this figure, the dimensionless parameters were $W_i = 0.2$, $\beta = 0.5$ and $\epsilon = 0.5$ and the spacing mesh was $\delta x = \delta y = 0.025$ to capture the details about the contour lines. We can note in these figures that the contours of the first normal stress difference $T^{xx} - T^{yy}$, and shear stress T^{xy} predicted by the PTT-AESM are in quite good agreement with the classical differential PTT model.

Another comparison between algebraic and differential models is displayed on Fig. 3

Table 2: Processing time for each simulation on every mesh. Read units as hour:minute:second.

Simulations	Mesh	Algebraic	Differential
S1	M1	00:00:15	00:00:15
	M2	00:02:02	00:02:05
	M3	00:19:08	00:21:33
	M4	07:03:28	09:39:38
	M5	29:41:51	–
S2	M1	00:00:17	00:00:16
	M2	00:02:07	00:02:17
	M3	00:19:36	00:20:21
	M4	06:15:33	11:39:40
	M5	30:34:39	–
S3	M1	00:00:18	00:00:15
	M2	00:02:51	00:01:56
	M3	00:20:53	00:20:54
	M4	07:58:42	08:48:42
	M5	29:12:33	–

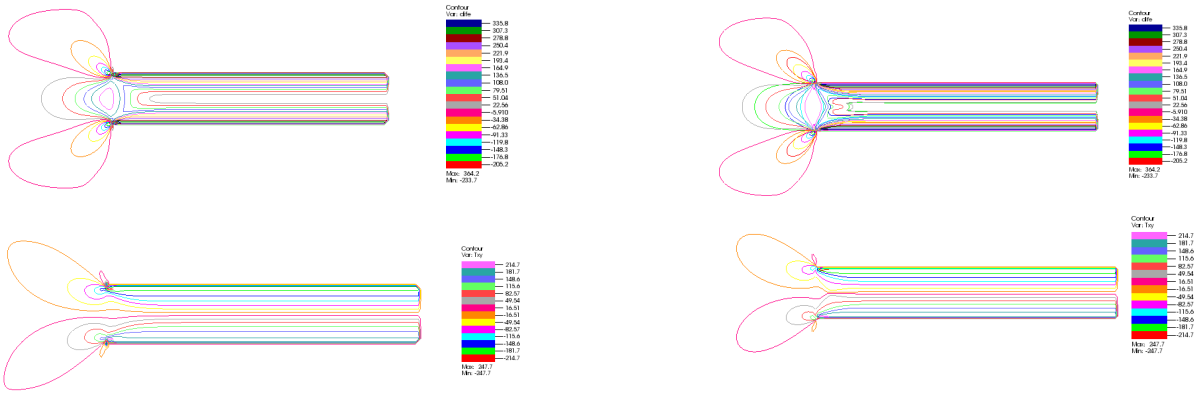

(a) PTT Differential Model. (b) PTT Algebraic Model.

Figure 2: Contour of the differential PTT and algebraic PTT-AESM models. First row: first normal stress difference ($T^{xx} - T^{yy}$). Second row: shear stress T^{xy}.

which exhibits the values of the components of the velocity (u and v) and non-Newtonian extra-stress tensor components on the horizontal centreline of the planar contraction. For Fig. 3, a coarse mesh was considered ($\delta x = \delta y = 0.05$).

For this case, the PTT-AESM predicts correctly the profiles of velocities and extra-stresses. However, some differences can be observed in the region of the abrupt contrac-

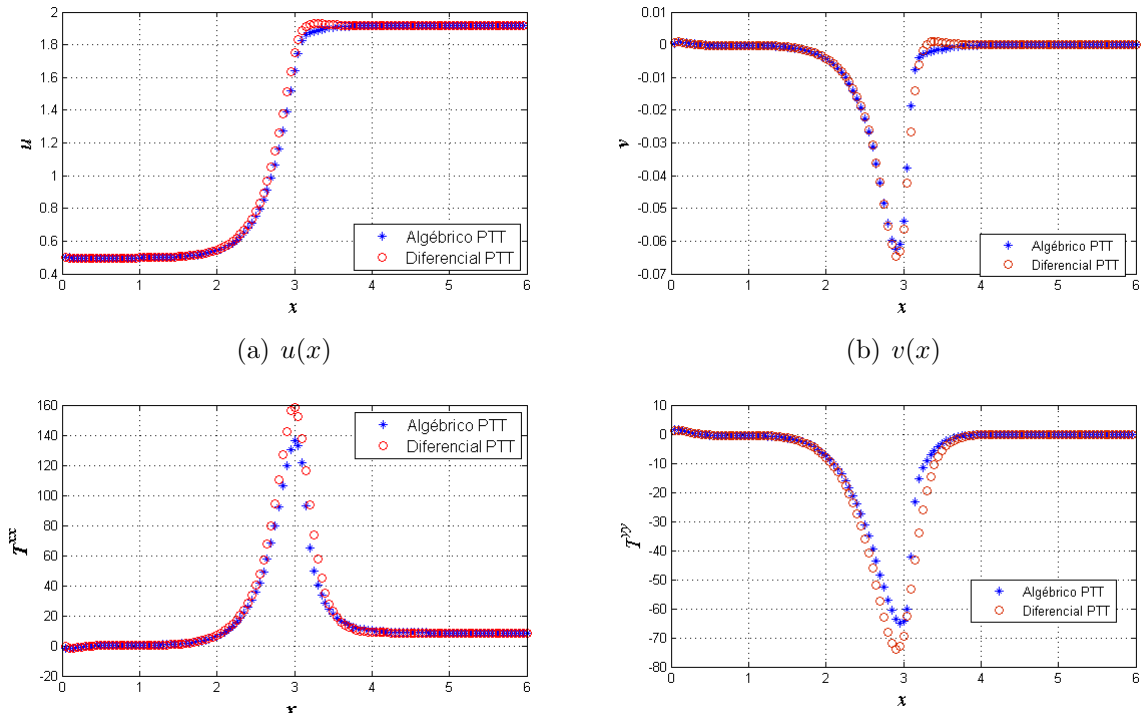

(a) $u(x)$ (b) $v(x)$

(c) $T^{xx}(x)$ (d) $T^{yy}(x)$

Figure 3: Comparisons between algebraic and differential models considering the values of the components u (a), v (b), T^{xx} (c) and T^{yy} (d) on the horizontal centreline of the planar contraction.

tion at $x = 3$. In this region, the PTT-AESM underpredict the normal stress, and the maximum difference is about 7 % for T^{xx} and 13 % for T^{yy}.

4.2.1 The influence of the parameter β

In this section the influence of the parameter β over the algebraic model (PTT-AESM) predictions is verified. The parameter β is defined as $\beta = \eta_S/\eta_0$, representing the ratio between the solvent viscosity and the total viscosity ($\eta_0 = \eta_S + \eta_P$). Taking the numerical solutions from PTT differential model as reference, the study is carry out using two values of $\beta = 0.5$ and 0.9. For this case, Re =1.0e-2, $Wi = 0.32$, $\epsilon = 0.5$, and the spacing mesh considered was $\delta x = \delta y = 0.05$.

In Fig. 4 we see clearly that the PTT-AESM can cope with the variation of β, predicting correctly the profiles of velocities and extra-stresses. It is also shown that when the parameter β increases, the difference between the predictions the normal stress given by the differential PTT and the PTT-AESM decreases.

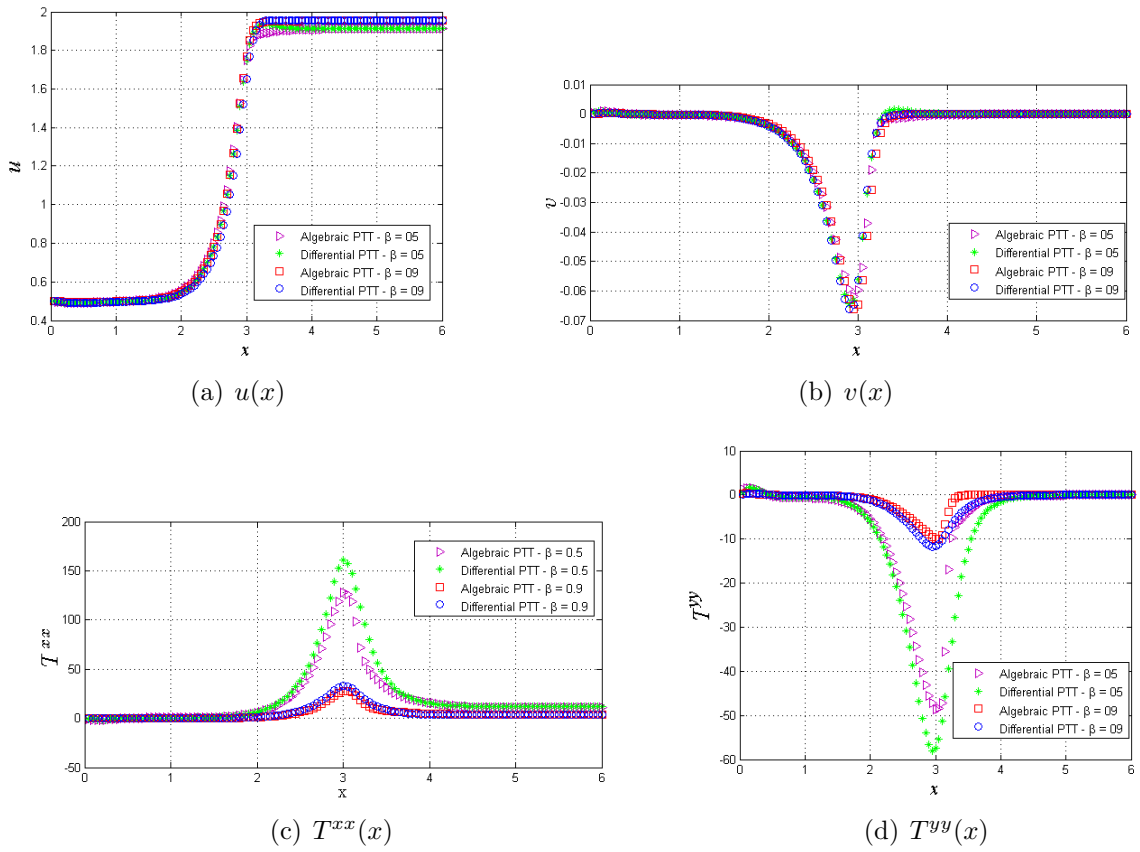

(a) $u(x)$ (b) $v(x)$

(c) $T^{xx}(x)$ (d) $T^{yy}(x)$

Figure 4: Comparisons between algebraic and differential models varying the parameter β considering the values of the components u (a), v (b), T^{xx} (c) and T^{yy} (d) on the horizontal centreline of the planar contraction.

4.2.2 The influence of the parameter ε

Following the same ideas of the previous section, in this section a brief study about the influence of the parameter ε over the algebraic model is done. The study is done considering two values of $\varepsilon = 0.4$ and 0.8. For this case, Re =1.0e-2, $Wi = 0.32$, $\beta = 0.5$, and the spacing mesh considered was $\delta x = \delta y = 0.05$.

We can observe that the PTT-AESM predicts correctly the profiles of velocity and extra-stress under the variation of the parameter ε from the PTT model. The maximum difference observed was in the critical region (abrupt entry of the contraction at $x = 3$) for the normal stress T^{xx} (18 %), for the case when $\varepsilon = 0.4$.

5 CONCLUSIONS

This work presented numerical studies for two problems, fully-developed channel flow and the flow through a 4:1 planar contraction at low Reynolds number, using the PTT algebraic model proposed by Mompean [2]. The accuracy and convergence of the numer-

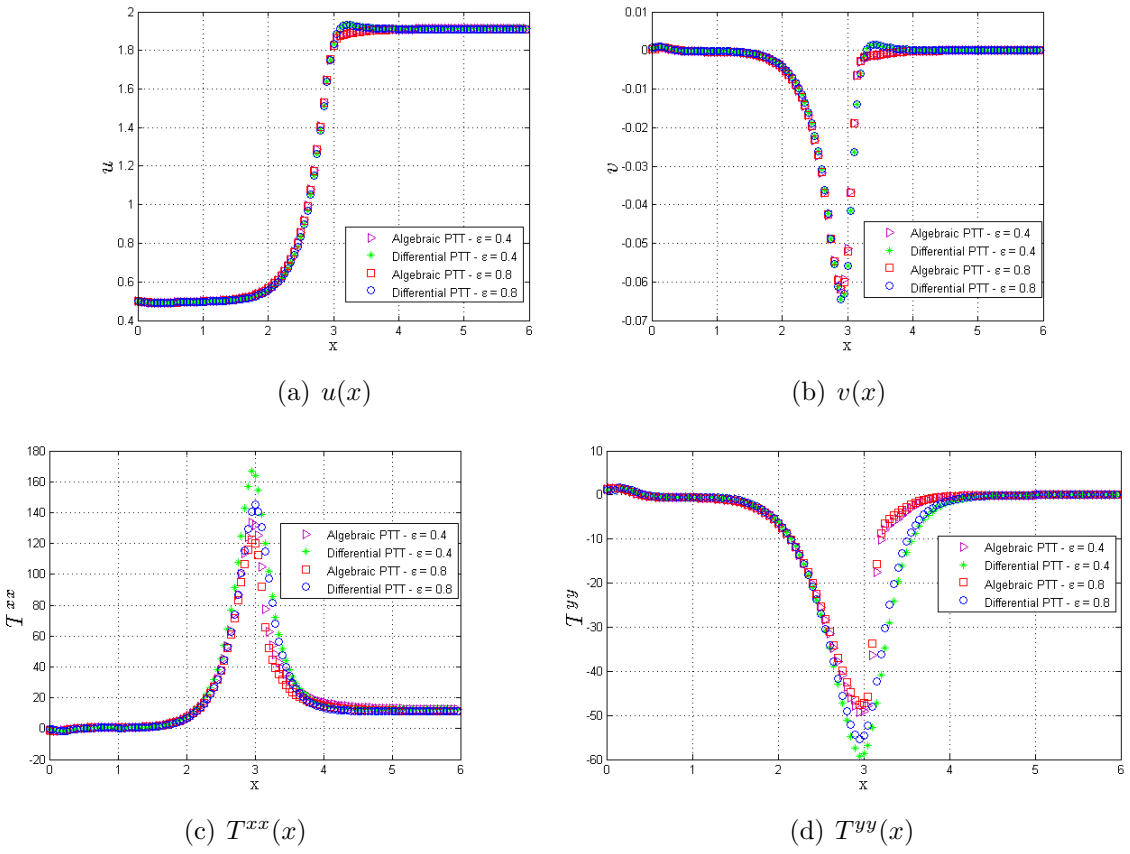

(a) $u(x)$ (b) $v(x)$

(c) $T^{xx}(x)$ (d) $T^{yy}(x)$

Figure 5: Comparisons between algebraic and differential models varying the parameter ε considering the values of the components u (a), v (b), T^{xx} (c) and T^{yy} (d) on the horizontal centreline of the planar contraction.

ical methodology was studied by the fully-developed channel flow problem using mesh refinements and analytic solutions. The numerical results were in excellent agreement with analytic solutions, presenting order approximately 2 in space, as it was expected according to the discretization of the equations. Moreover, in this problem the cpu time of the algebraic model was smaller than the same predictions of the differential model, when refined meshes had been considered. Moreover, on the finer grid only the PTT algebraic methodology converged. For the complex flow through a 4:1 planar contraction at low Reynolds number, the PTT-AESM was able to predict correctly velocities and extra-stresses, and cope with the variation of important parameters in the numerical simulation of PTT fluids, i. e. the ratio β between the solvent and the total viscosity and the parameter ε. For the cases studied in this work the maximum difference observed between the PTT-AESM and the classical PTT differential constitutive equation was about 18 % in the critical region of abrupt entry of the 4:1 contraction. Future studies for higher Reynolds and Weissemberg numbers will be carried out.

REFERENCES

[1] Phan-Thien, N. and Tanner, R.I. A new constitutive equation derived from network theorys. *J. Non-Newt. Fluid Mech.* (1977) **2**:353–365.

[2] Mompean, G. On predicting abrupt contraction flows with differential and algebraic viscoelastic models. *Comput. Fluids* (2002) **31**:935–956.

[3] Tomé, M.F. and McKee, S. GENSMAC: a computational marker-and-cell method for free surface flows in general domains. *J. Comput. Phys.* (1994) **110**:171–186.

[4] Mompean, G. and Jongen, T. and Gatski, T. and Deville, M. n algebraic extra-stress models for the simulation of viscoelastic flows. *J. Non-Newt. Fluid Mech.* (1998) **79**:261–281.

[5] Bird, R.B. and Armstrong, R.C. and Hassager, O. *Dynamics of Polymetric Liquids. Fluid Mechanics*. Wiley, Vol. I., (1977).

[6] Bird, R.B. and Curtiss, C.F. and Armstrong, R.C. and Hassager, O. *Dynamics of Polymetric Liquids. Kinetic Theory*. Wiley, Vol. II., (1987).

[7] McKee, S. and Tomé, M.F. and Ferreira, V.G. and Cuminato, J.A. and Castelo, A. and Sousa, F.S. and Mangiavacchi, N. The MAC Method. *Comput. Fluids* (2008) **37**:907–930.

[8] Oishi, C.M. and Martins, F.P. and Tomé, M.F. and Cuminato, J.A. and McKee, S. Numerical solution of the eXtended PomPom model for viscoelastic free surface flows. *J. Non-Newt. Fluid Mech.* (2011) **166**:165–179.

[9] Paulo, G.S. and Oishi, C.M. and Tomé, M.F. and Alves, M.A. and Pinho, F.T. Numerical solution of the FENE-CR model in complex flows. *J. Non-Newt. Fluid Mech.* (2014) **204**:50–61.

[10] Alves, M. and Oliveira, P.J. and Pinho, F.T. A convergent and universally bounded interpolation scheme for the treatment of advection. *Int. J. Num. Meth. Fluids* (2003) **41**:47–75.

[11] D. O. A. Cruz and F. T. Pinho Analytical solutions for fully developed laminar flow of some viscoelastic liquids with a Newtonian solvent contribution. *J. Non-Newt. Fluid Mech.* (2005) **132**:28–35.